Excitation by scattering/total field decomposition and Uniaxial PML in the geometric formulation

Matteo Cicuttin[1], Lorenzo Codecasa[2], Ruben Specogna[1], Francesco Trevisan[1]

[1] Università di Udine, Dip. di Ingegneria Elettrica, Gestionale e Meccanica, I-33100, Udine, Italy
[2] Politecnico di Milano, Dip. di Elettronica, Informazione e Bioingegneria, I-20133, Milano, Italy

The paper presents a general technique to apply excitations in the framework of discrete geometric numerical methods using dual grids, like DGA (Discrete Geometric Approach) and FIT (Finite Integration Technique). The technique overcomes some limitations of the *impedance boundary condition* we proposed in a previous work, especially when dealing with waveguides, where specific excitation modes must be applied. The proposed approach is based on a scattering/total field decomposition which, if needed, allows to study scatterings due to objects.

***Index Terms*—Discrete Geometric Approach, Finite Integration Technique, Waveguide, Modal Excitation, Port boundary condition.**

I. Introduction

IN OUR PREVIOUS work [1] it was shown how a *plane wave* excitation can be integrated in the framework of the Discrete Geometric Approach (DGA). The purpose was attained by using an *impedance boundary condition* which allowed to simulate the plane wave. This kind of excitation, however, finds limited application in simulating waveguides. In particular it can be applied only at waveguide ports where the contributions of high-order modes can be neglected, otherwise different impedance of the modes will cause reflections. When multiple modes are present, a more general approach is required. A possible technique is to split the domain in a scattering region Ω_s and a total region Ω_t, and apply the excitation at the interface Σ between these two regions. Reflections due to the domain truncation are avoided by terminating the two regions with Uniaxial PMLs (UPMLs) [2], as depicted in Fig. 1. An advantage of this kind of arrangement is that it allows the presence of objects producing scatterings in the surroundings of the interface Σ. In addition, if only scattered field or total field are needed, the parts of Ω_t or Ω_s which are not PML can be omitted without compromising the effectiveness of the method. The excitation is applied on the *interface* Σ between Ω_s and Ω_t by means of a *dual boundary grid* [8], [9]. In this paper it is shown how this technique can be extended to FIT [4], DGA [3], Cell Method [5] and other methods involving dual cell complexes. To this aim the following the discussion will be focused on a piece of rectangular waveguide but the technique can be applied to guides of arbitrary shape. After a brief description of the discrete electromagnetic wave propagation problem, we will discuss the scattering field/total field decomposition. In particular we will show that Maxwell's equations and constitutive relations must be modified to account for the excitation contribution imposed on Σ. A subsequent section is devoted to the discussion on how the excitation is actually specified and finally the results of a couple of numerical experiments are shown.

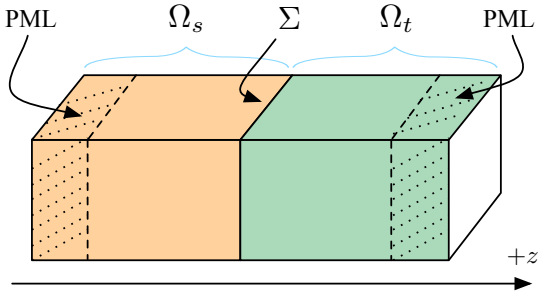

Fig. 1. The subregions of the problem: PMLs, scattered field region Ω_s and total field region Ω_t. Excitation is applied on the interface Σ.

II. Electromagnetic wave propagation in frequency domain

The time-harmonic electromagnetic wave propagation in a region of space Ω is described in terms of the usual Maxwell differential formulation [6] as

$$\nabla \times (\boldsymbol{\nu} \nabla \times \boldsymbol{e}) - \omega^2 \boldsymbol{\epsilon} \boldsymbol{e} = \boldsymbol{0}, \tag{1}$$

where $\boldsymbol{\nu}$ and $\boldsymbol{\epsilon}$ are the material tensors, ω is the angular frequency and $\boldsymbol{e}$ is an unknown complex-valued vector function describing the electric field. Numerical treatment of (1) requires the discretization of Ω, which is obtained by means of a *primal* tetrahedral grid $\mathcal{G}$ and a *dual* grid $\tilde{\mathcal{G}}$ induced by the barycentric subdivision of $\mathcal{G}$. Some integral electromagnetic quantities are associated with these interlocked grids, as prescribed by the DGA method. In particular

- Electromotive force U_k to edges $e_k \in \mathcal{G}$;
- Magnetic flux Φ_k to faces $f_k \in \mathcal{G}$;
- Magnetomotive force F_k to edges $\tilde{e}_k \in \tilde{\mathcal{G}}$;

Manuscript received December 1, 2012; revised September 17, 2014. Corresponding author: M. Cicuttin (email: matteo.cicuttin@uniud.it).
Color versions of one or more of the figures in this paper are available online at http://ieeexplore.ieee.org.
Digital Object Identifier 10.1109/TMAG.2013.2281076

- Electric flux Ψ_k to faces $\tilde{f}_k \in \tilde{\mathcal{G}}$.

These quantities are stored in the corresponding arrays $\mathbf{U}$, $\mathbf{\Phi}$, $\mathbf{F}$ and $\mathbf{\Psi}$ containing electromotive forces, magnetic fluxes, magnetomotive forces and electric fluxes for the whole mesh, respectively. By introducing the face-edge incidence matrix $\mathbf{C}$ discrete Maxwell's equations can be written, in particular the discrete Ampère–Maxwell law is written as

$$\mathbf{C}^T\mathbf{F} = i\omega\mathbf{\Psi}, \tag{2}$$

while the discrete Faraday–Neumann law as

$$\mathbf{C}\mathbf{U} = -i\omega\mathbf{\Phi}. \tag{3}$$

Primal quantities and dual quantities are related by the constitutive relations

$$\mathbf{\Psi} = \mathbf{M}_\epsilon\mathbf{U}, \tag{4}$$

$$\mathbf{F} = \mathbf{M}_\nu\mathbf{\Phi}, \tag{5}$$

where $\mathbf{M}_\nu$ and $\mathbf{M}_\epsilon$ are the constitutive matrices, which are built as prescribed by the energetic approach for tetrahedra [7]. Some algebraic manipulation of (2), (3), (4) and (5) yields the discrete wave propagation problem in the frequency domain

$$\mathbf{C}^T\mathbf{M}_\nu\mathbf{C}\mathbf{U} - \omega^2\mathbf{M}_\epsilon\mathbf{U} = \mathbf{0}, \tag{6}$$

which is the discrete counterpart of problem (1).

III. Scattered field/Total field formulation

The electromagnetic field computed in the Ω_t region is the sum of the field due to the excitation imposed on Σ and, if scattering objects are present in Ω_t, the field due to the reflections produced by the scatterer (Fig. 2). On the other hand, the scattering field in the region Ω_s is only due to the reflections occurring in Ω_t returning back to Ω_s. In both regions wave propagation occurs as prescribed by (1), but on Σ a transition from the total field to the scattered field happens. The transition is obtained by "adding" the excitation contribution on the boundary primal and dual edges on Σ. This is better explained by thinking the scattering field region and total field region as separated (Fig. 2). In this way the boundary Σ is split in two, a part pertaining to Ω_t and a part pertaining to Ω_s. On the Ω_s side, electromotive and magnetomotive forces on the edges of Σ can be decomposed in an excitation component and a scattering component. At the same time, the electromagnetic quantities on the Ω_t side of Σ must be constrained to be equal to the ones associated to the corresponding edges of the Ω_s side. This requires the modification of the Ampère–Maxwell law, the Faraday–Neumman law and the constitutive relations in the volume elements of Ω_s touching Σ as explained in the subsequent sections. In the following, local laws are described (which involve local quantities denoted with the superscript v) and then it is shown how local laws are used to derive the global problem. For clarity of notation, the superscript v is omitted from incidence matrices: when used with local quantities, $\mathbf{C}$ and $\mathbf{C}^T$ are considered to be the local incidence matrices, otherwise they are considered to be the global ones.

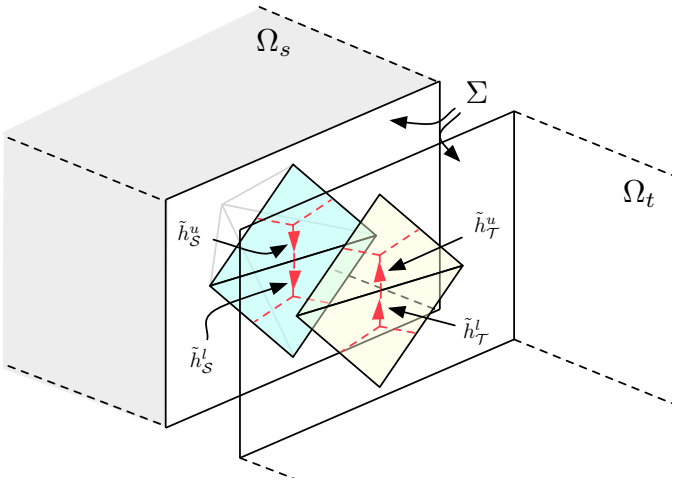

Fig. 2. Boundary primal edges e^Σ_k and dual edges $\tilde{e}^\Sigma_k$ introduced in the interface between total field and scattered field regions.

A. Ampère–Maxwell law

The Ampère–Maxwell law involves the edges of the *boundary dual grid* $\tilde{\mathcal{G}}^\Sigma$ on Σ. The boundary dual edges $\tilde{e}^\Sigma_{\mathcal{T}}$ and $\tilde{e}^\Sigma_{\mathcal{S}}$ are depicted in Fig. 2 as dashed lines. Each edge lies within two tetrahedra and can be split in *half edges*, such that $\tilde{e}^\Sigma_{\mathcal{T}} = \tilde{h}^u_{\mathcal{T}} \cup \tilde{h}^l_{\mathcal{T}}$ and $\tilde{e}^\Sigma_{\mathcal{S}} = \tilde{h}^u_{\mathcal{S}} \cup \tilde{h}^l_{\mathcal{S}}$ (Fig. 2). Each half edge belongs to a single tetrahedron, for example $\tilde{h}^u_{\mathcal{T}}$ belongs to the upper tetrahedron in $\Omega_{\mathcal{T}}$ while $\tilde{h}^l_{\mathcal{S}}$ belongs to the lower tetrahedron in $\Omega_{\mathcal{S}}$ (Fig. 2). The half edge quantities contribute to the local Ampère–Maxwell law of a single tetrahedron v.

Considering for example the two upper tetrahedra in Fig. 2, it can be observed that the magnetomotive force $F_{\mathcal{T}}$ on $\tilde{h}^u_{\mathcal{T}}$ and $F_{\mathcal{S}}$ on $\tilde{h}^u_{\mathcal{S}}$ must satisfy the relation $F^\Sigma_{\mathcal{T}} + F^\Sigma_{\mathcal{S}} = 0$ because $\tilde{h}^u_{\mathcal{T}}$ and $\tilde{h}^u_{\mathcal{S}}$ are in fact the same edge but with opposite orientation. Moreover, on the Ω_s side, which is where the excitation is applied, the magnetomotive force $F_{\mathcal{S}}$ can be further decomposed in the unknown scattered contribute $F_{\mathcal{S}s}$ and in the known radiated contribute $F_{\mathcal{S}r}$. This implies that the balance of the magnetomotive forces must satisfy the condition $F_{\mathcal{T}} + F_{\mathcal{S}s} = -F_{\mathcal{S}r}$. Thus, the local Ampère–Maxwell law for a tetrahedron v in $\Omega_{\mathcal{S}}$ touching Σ is written as

$$\mathbf{C}^T\mathbf{F}^v - \mathbf{F}^v_r = i\omega\mathbf{\Psi}^v, \tag{7}$$

where the $\mathbf{F}^v$ term collects the circulation of the magnetomotive force in the inner edges of Ω_s, while the $\mathbf{F}^v_r$ term collects the magnetomotive forces on the half edges of v due to the excitation.

B. Faraday–Neumann law

The Faraday–Neumann law involves primal edges and faces of elements lying on the Ω_s side of Σ. An element can touch Σ with a node, with an edge or with an entire face. The first case is of no interest since no nodal quantities are involved in Faraday–Neumann law, while the second one is only a particularization of the third case. The third case is then analyzed.

Let $f_1, \ldots, f_4$ be the faces of a volume element v and $\mathbf{\Phi}^v = (\phi_1^v, \ldots, \phi_4^v)$ the array of the magnetic fluxes across them. Without loss of generality we assume that the face on Σ is f_1, so $v \cap \Sigma = f_1$. Moreover, assume also that the edges surrounding f_1 are e_1, e_2, e_3. The electromotive forces U_1^v, U_2^v, U_3^v on e_1, e_2, e_3 and the flux ϕ_1^v on f_1 can be decomposed in an unknown scattering component and in a known radiated component, obtaining $U_k^v = U_{k,s}^v + U_{k,r}^v$ with $k \in \{1, 2, 3\}$ and $\phi_1^v = \phi_{1s}^v + \phi_{1r}^v$. The Faraday–Neumann law can be rewritten as follows:

$$\mathbf{C} \begin{pmatrix} U_{1s}^v + U_{1r}^v \\ U_{2s}^v + U_{2r}^v \\ U_{3s}^v + U_{3r}^v \\ U_4^v \\ U_5^v \\ U_6^v \end{pmatrix} = -i\omega \begin{pmatrix} \phi_{1s}^v + \phi_{1r}^v \\ \phi_2^v \\ \phi_3^v \\ \phi_4^v \end{pmatrix}. \tag{8}$$

By separating known and unknown quantities and writing the equation in compact form we obtain

$$\mathbf{C}\left(\mathbf{U}_r^v + \mathbf{U}_s^v\right) = -i\omega\left(\mathbf{\Phi}_r^v + \mathbf{\Phi}_s^v\right). \tag{9}$$

C. Constitutive relations

A reasoning similar to the one carried out for the Faraday–Neumann law applies for the constitutive relations when writing them for the elements on the Ω_s side touching Σ. Using the setting of the previous section, electromotive forces are split in scattered and radiated contributions

$$\mathbf{\Psi}^v = \mathbf{M}_\epsilon^v \begin{pmatrix} U_{1s}^v + U_{1r}^v \\ U_{2s}^v + U_{2r}^v \\ U_{3s}^v + U_{3r}^v \\ U_4^v \\ U_5^v \\ U_6^v \end{pmatrix} = \mathbf{M}_\epsilon^v \begin{pmatrix} U_{1s}^v \\ U_{2s}^v \\ U_{3s}^v \\ U_4^v \\ U_5^v \\ U_6^v \end{pmatrix} + \mathbf{M}_\epsilon^v \begin{pmatrix} U_{1r}^v \\ U_{2r}^v \\ U_{3r}^v \\ 0 \\ 0 \\ 0 \end{pmatrix}. \tag{10}$$

The magnetic constitutive equation, on the other hand, has to be used only when a tetrahedron of the Ω_s side is in contact with Σ by a face, since it involves only face quantities. Again, magnetic fluxes are split in scattered and radiated contributions

$$\mathbf{F}^v = \mathbf{M}_\nu^v \begin{pmatrix} \phi_{1s}^v + \phi_{1r}^v \\ \phi_2^v \\ \phi_3^v \\ \phi_4^v \end{pmatrix} = \mathbf{M}_\nu^v \begin{pmatrix} \phi_{1s}^v \\ \phi_2^v \\ \phi_3^v \\ \phi_4^v \end{pmatrix} + \mathbf{M}_\nu^v \begin{pmatrix} \phi_{1r}^v \\ 0 \\ 0 \\ 0 \end{pmatrix}. \tag{11}$$

Written in compact form, the two constitutive relations become

$$\mathbf{\Psi}^v = \mathbf{M}_\epsilon^v(\mathbf{U}_s^v + \mathbf{U}_r^v), \tag{12}$$

$$\mathbf{F}^v = \mathbf{M}_\nu^v(\mathbf{\Phi}_s^v + \mathbf{\Phi}_r^v). \tag{13}$$

D. Problem assembly

Consider (7), (9), (12) and (13): by solving (7) for the quantity $(\mathbf{\Phi}_r^v + \mathbf{\Phi}_s^v)$ then substituting (12), (7), (13) and rearranging, the expression

$$\mathbf{K}^v\mathbf{U}_s^v = -\mathbf{K}^v\mathbf{U}_r^v - i\omega\mathbf{F}_r^v \tag{14}$$

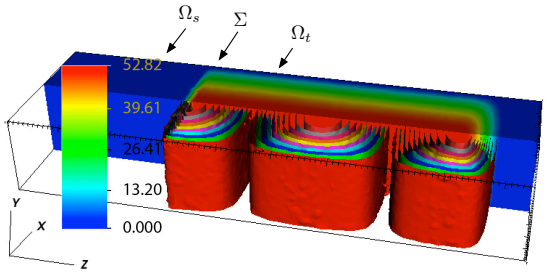

Fig. 3. The waveguide subject of the simulation is depicted, including PMLs, scattering region Ω_s and total field region Ω_t. The TE_{10} mode excitation is applied on Σ. Dimensions are given in text. Scale shows the magnitude of the electric field in V/m (solid color region).

is obtained, where $\mathbf{K}^v = \mathbf{C}^T\mathbf{M}_\nu^v\mathbf{C} - \omega^2\mathbf{M}_\epsilon^v$. Assembling element by element in the usual way, the equation

$$\mathbf{K}\mathbf{U} = -\mathbf{K}\mathbf{U}_r - i\omega\mathbf{F}_r \tag{15}$$

is obtained, where all the matrices involved are *global*. The unknowns $\mathbf{U}_s^v$ from (14) are now part of the unknown $\mathbf{U}$ in (15) and appear in the positions corresponding to the primal edges of Σ. Moreover, the terms $\mathbf{U}_r$ and $\mathbf{F}_r$ are nonzero only in correspondence of the primal edges of Σ and the dual edges of Σ respectively.

IV. Application of the Excitation on the Interface

At this point, applying the desired excitation is a matter of setting the correct values for the electromotive and magnetomotive forces on both the primal and dual edges of Σ by fixing the values of $U_{k,i}$ and $F_{k,i}$. In the case of the rectangular waveguide of the example, these quantities are calculated by integrating on primal and dual mesh edges the field computed with the usual closed-form equations for TE and TM modes. Conversely, in the case of an arbitrary shape of the waveguide, the values of $U_{k,i}$ and $F_{k,i}$ are computed by solving a 2D eigenvalue problem on Σ. We consider Σ planar, but the method can be applied also to curved surfaces by introducing an artificial plane boundary.

V. Numerical Experiments

The presented technique was implemented in EMT, our DGA workbench code written in C++14. The simulations were performed on Mac OS X 10.9.5 running on a Core i7 3615QM with 16 GB of RAM, Clang/LLVM 3.5 compiler and MKL PARDISO solver. To test the technique two numerical experiments were prepared. The first one was the simulation of a section of rectangular waveguide (Fig. 3), discretized with a mesh that included 178280 tetrahedra yelding a problem of 192242 unknowns.

Such a toy problem was useful to check the correctness of the results against analytical solutions. In this case assembly took 1.84 seconds while solver took 6.44 seconds. The waveguide dimensions were $a = 60$mm (in x direction) and $b = 30$mm (in y direction), which give a cutoff frequency for the TE_{10} mode of about 2.5 GHz. PML regions length was 30mm, and were implemented according to the Uniaxial PML

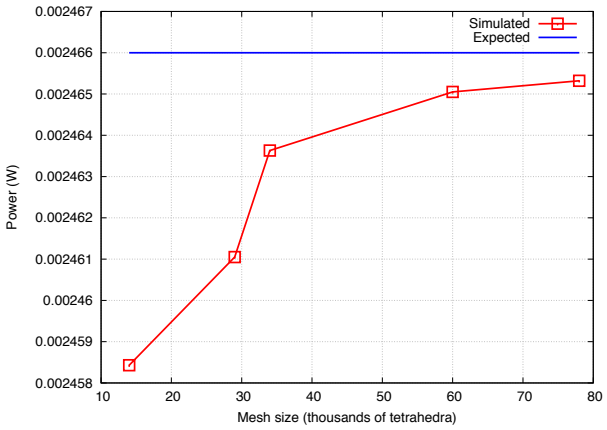

Fig. 4. Problem 1: Mesh size (number of tetrahedra) vs. power flowing in Ω_t towards positive z. Simulated power is compared with expected theoretical power.

technique, as described in [2]. The length of scattered field region was 30mm and waveguide (total field) region length was 100mm. Finally, the operating frequency was $f = 3.8$ GHz. The computed field configuration was in accordance with analytic problem solution. As an additional test, power flowing in Σ was computed for different mesh sizes (Fig. 4). The flux of the poynting vector on the interface Σ is computed as [3]

$$P = \frac{1}{2}\mathbf{U}_\Sigma^T \mathbf{F}_\Sigma^*, \tag{16}$$

where the arrays $\mathbf{U}_\Sigma$ and $\mathbf{F}_\Sigma$ are respectively the electromotive and magnetomotive forces on the edges of Σ.

As a second example, a perfectly conductive sphere of radius $r = 5$mm was placed inside the waveguide of the previous example, near the port providing the TE_{10} excitation (Fig. 5). In this case operating frequency was $f = 4.7$ GHz. The reflections due to the scatterer are visible in the Ω_s region depicted in (Fig. 5) together with the transition from the total field to the scattered field.

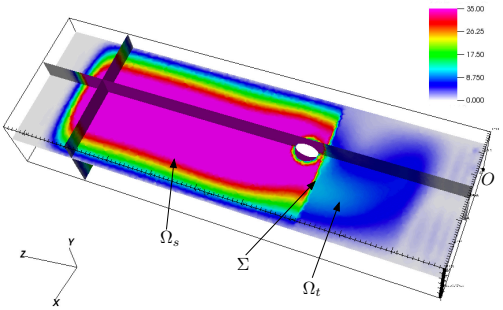

Fig. 5. Scattering field produced in Ω_s by a perfectly conductive sphere of radius $r = 5$mm, placed off-center ($x = 25$mm, $y = 20$mm, $z = 67$mm, origin marked O) near the port.

The proposed approach was validated against a highly accurate in-house developed FEM code (Fig. 6) of the second order and using edge-elements. Our approach has the advantage that, unlike FEM, it provides a strong geometrical foundation for the treatment of boundary and interface conditions. The advantage is given by the boundary dual grids (Fig. 2), which allow manipulation of all quantities related to the boundaries of the simulation domain without using interpolation [1], [3], [8], [9].

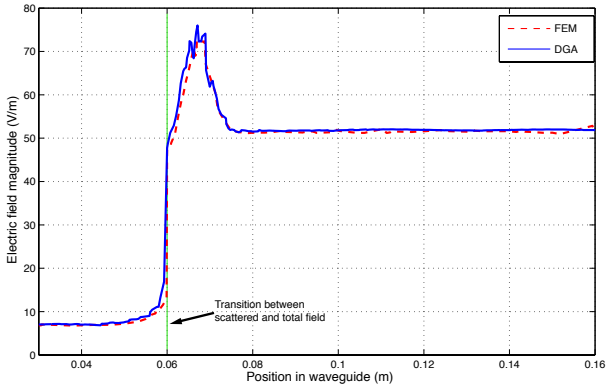

Fig. 6. Problem 2: The technique was compared against a FEM code. The magnitude of electric field in the scattering and total regions (excluding PML parts) is depicted. Electric field was sampled in the line extending from (0.03, 0.015, 0.03) to (0.03, 0.015, 0.16).

VI. Conclusions

A novel technique for the application of excitations on the boundaries of the simulation domain was added to the DGA framework. The technique allows to apply the correct excitations to waveguides, a case where our previous work [1] was of limited applicability. Total/scattered field decomposition, together with the use of Perfectly Matched Layers, allowed to overcome the limitations. Moreover, scattering objects near the scattering/total transition are correctly handled.

Acknowledgements

This work was supported by the PAR FSC 2013 EMCY project of Friuli Venezia Giulia region, Italy.

References

[1] S. Chialina, M. Cicuttin, L. Codecasa, R. Specogna, F. Trevisan, "Plane wave excitation for frequency domain electromagnetic problems by means of impedance boundary condition", *IEEE Trans. Magn.*, Vol. 51, No. 3, 2015.

[2] A. Taflove, *Advances in Computational Electrodynamics,* Artech House Publishers, Boston, 1998

[3] L. Codecasa, R. Specogna, F. Trevisan, "Discrete Geometric Formulation of Admittance Boundary Conditions for Frequency Domain Problems Over Tetrahedral Dual Grids", *IEEE Trans. Antennas Propagat.*, vol. 60, no. 8, pp. 3998–4002, 2012.

[4] M. Clemens, T. Weiland, "Discrete electromagnetism with the finite integration technique", *PIER*, Vol. 32, pp. 65-87, 2001.

[5] E. Tonti, "Why starting from differential equations for computational physics?", *J. Comput. Phys.*, Vol. 257, Part B, pp. 1260-1290, 2014.

[6] R. E. Collin, *Foundations for Microwave Engineering (Second edition)*, McGraw-Hill International Editions, New York, 1992.

[7] L. Codecasa, R. Specogna, F. Trevisan, "Symmetric Positive-Definite Constitutive Matrices for Discrete Eddy-Current Problems", *IEEE Trans. Magn.*, Vol. 43, No. 2, pp. 510–515, 2007.

[8] B. Auchmann, S. Kurz, *The pairing matrix in discrete electromagnetism*, Eur. Phys. J. Appl. Phys., vol. 39, no. 2, pp. 133–141, Jun. 2007.

[9] L. Codecasa, "*Refoundation of the Cell Method by means of Augmented Dual Grids*", *IEEE Trans. Magn.*, Vol. 50, No. 2, pp. 497–500, 2014.